

Structural, elastic, electronic and magnetic properties of quaternary Heusler alloy $\text{Cu}_2\text{MnSi}_{1-x}\text{Al}_x$ ($x = 0 - 1$): First-principles study

B. Benichou^{a,b,*}, Z. Nabi^c, B. Bouabdallah^d and H. Bouchenafa^{a,e}

^aDepartment of Physics, Faculty of Sciences Exact,
Djillali Liabès University, Sidi Bel Abbès 22000, Algeria.

^bDepartment of Electronics, Faculty of Technology,
Hassiba Benbouali University, Chlef 02000, Algeria.

^cLaboratory of Catalysis and Reactive Systems,
Physics Department, Djillali Liabès University, Sidi Bel Abbès 22000, Algeria.

^dCondensed Matter and Sustainable Development Laboratory, Djillali Liabès University,
Sidi Bel Abbès 22000, Algeria.

^eDepartment of Physics, Faculty of Sciences Exact and Informatics,
Hassiba Benbouali University, Chlef 02000, Algeria.
e-mail: boucif.benichou@yahoo.fr

Received 27 November 2017; accepted 19 December 2017

We investigate the structural, elastic, electronic and magnetic properties of the Heusler compounds Cu_2MnSi , Cu_2MnAl and $\text{Cu}_2\text{MnSi}_{1-x}\text{Al}_x$ quaternary alloys, using the full-potential linear-augmented plane-wave method (FP-LAPW) in the framework of the density functional theory (DFT) using the generalized gradient approximation of Perdew-Burke-Ernzerhof (GGA-PBE). Our results provide predictions for the quaternary alloy $\text{Cu}_2\text{MnSi}_{1-x}\text{Al}_x$ ($x = 0.125, 0.25, 0.375, 0.5$) in which no experimental or theoretical data are currently available. We calculate the ground state's properties of $\text{Cu}_2\text{MnSi}_{1-x}\text{Al}_x$ alloys for both nonmagnetic and ferromagnetic configurations, which lead to ferromagnetic and metallic compounds. Also, the calculations of the elastic constants and the elastic moduli parameters show that these quaternary Heusler alloys are ductile and anisotropic.

Keywords: Electronic structure; elastic properties; ab-initio calculations; quaternary Heusler alloys.

PACS: 75.10.Hk; 71.45.Nt

1. Introduction

So far, the Heusler alloys are still interesting due to their potential application in spintronics, such as giant magnetoresistance (GMR), tunneling magnetoresistance (TMR) [1], superconductors [2], ferromagnetic shape memory alloys [3] and magnetic actuator [4]. Besides of Heusler alloys, the intermetallic compounds are also promising materials for automobile, aviation, aerospace and advanced thermoelectric applications.

Many works on Cu_2MnZ , especially Cu_2MnAl alloys, have been investigated in both cases, experimentally [5-7] and theoretically [8-10]. Rai *et al.*, [11] showed that Cu_2MnAl is an interesting ferromagnetic and metallic compound in spite of its non-ferromagnetic elements. Hamri *et al.*, [12] illustrated that all the studied ferromagnetic systems X_2MnSn ($\text{X} = \text{Cu}, \text{Ni}, \text{Pd}$) exhibit a metallic character and possess an interesting elastic constants. Also, Ghosh *et al.*, [13] found that Cu_2MnGa has metallic and ferromagnetic properties and is thermodynamically as well as mechanically stable alloy. In addition to ternary Heusler studies, there exist several searches on quaternary alloys. Galaknakis [14] investigated quaternary alloys as $\text{X}_2\text{Y}_{1-x}\text{Y}'_x\text{Z}$, $(\text{X}_{1-x}\text{X}'_x)_2\text{YZ}$ and $\text{X}_2\text{YZ}_{1-x}\text{Z}'_x$, he found that there is a possibility of obtaining half-metallic systems. The spin polarization of $\text{Co}_2\text{Cr}_{1-x}\text{Fe}_x\text{Al}$ quaternary alloys have been re-

ported by Karthik *et al.*, [15]. Nanto *et al.*, [16] have studied the magnetic properties of nanocrystalline $\text{Fe}_2\text{Mn}_{0.5}\text{Cu}_{0.5}\text{Al}$ using mechanical alloying technique.

This paper is arranged as follows: In the next section, we give a brief description of the calculation method. Section 3 deals with the crystal structural aspects. In Sec. 4, the results and their comments are presented and the paper is ended after by a conclusion summarizing the study.

2. Computational Details

The first principles calculations performed within the FP-LAPW method [17] which is implemented in the WIEN2k code [18], based on the DFT theory [19,20], where the GGA approximation [21] has employed to describe the exchange and correlation potential. For the numerics, we estimate the plane wave parameter $R_{MT} \times K_{\max}$ as 7.0, and to ensure the correctness of the calculations, we have taken $l_{\max} = 12$. The G_{\max} parameter was 12.0. The separation energy between the core and the valence states has chosen as - 6.0 Ry. The self consistent potentials calculated on a $21 \times 21 \times 21$ k-mesh in the Brillouin Zone for ternary alloys and $2 \times 2 \times 2$ k-mesh for quaternary alloys, which correspond respectively, to 286 and 4 k-points in the irreducible BZ. The muffin-tin sphere radii were 2.2, 2.0, 2.0 and 1.9 for Cu, Mn, Si and Al,

respectively. The energy convergence criterion was taken as 10^{-5} Ry.

3. Crystal structure

Full-Heusler alloys have the chemical formula X_2YZ , where X and Y denote transition metals and Z is an s-p element. The atomic positions for X (Cu) atoms are $(1/4, 1/4, 1/4)$, $(3/4, 3/4, 3/4)$, while $(1/2, 1/2, 1/2)$ for Y (Mn) and for Z (Si, Al) it is $(0, 0, 0)$. In Fig. 1, we show the crystal structure of $Cu_2MnSi_{1-x}Al_x$ ($x = 0, 0.125, 0.25, 0.375, 0.5, 1$) alloys, where the present structures consist of four interpenetrating face-centered-cubic sublattices, with $L2_1$ phase and Fm-3m, space group no. 225. To simulate $Cu_2MnSi_{1-x}Al_x$ quaternary alloys, we consider a $(2 \times 2 \times 2)$ supercell eight times bigger than $L2_1$ unit cell. The supercell is then constituted of 32 atoms; 16 Cu, 8 Mn and 8 Si/Al, as shown in Fig. 1.

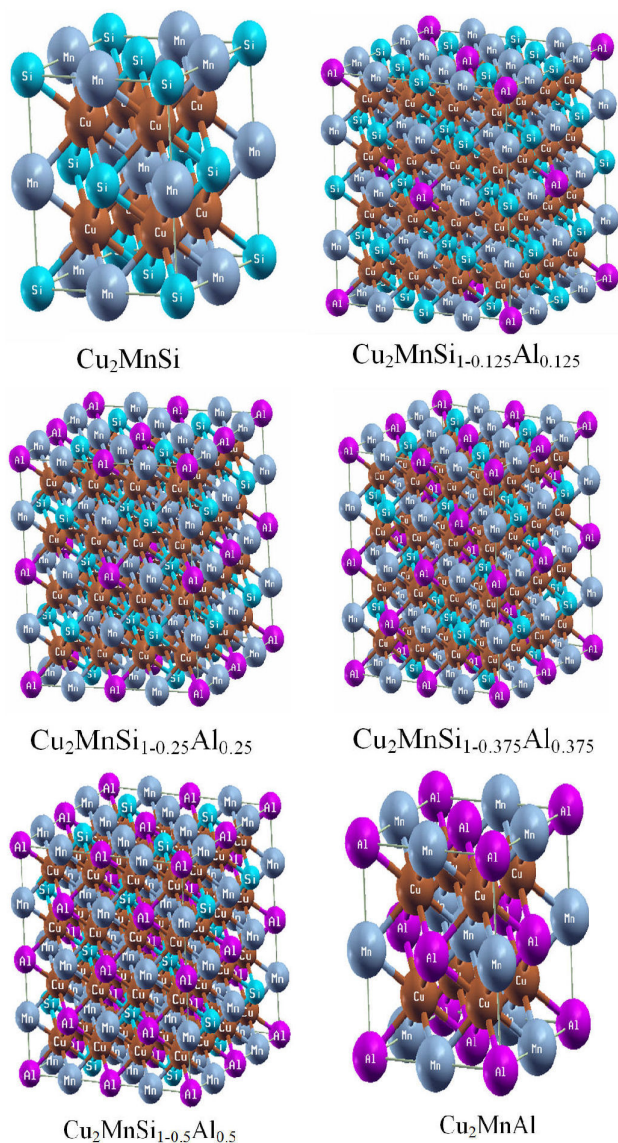


FIGURE 1. Crystal structure of $Cu_2MnSi_{1-x}Al_x$ ($x = 0, 0.125, 0.25, 0.375, 0.5, 1$).

4. Results and Discussion

4.1. Structural Properties

To obtain the lattice constant, the bulk modulus and its first pressure derivative which are listed in Table I, we have fitted the computed energies to the empirical Murnaghan's equation of state [22]. In this respect, the optimization of the geometrical structure parameters of $Cu_2MnSi_{1-x}Al_x$ alloys has performed by using nonmagnetic (NM) and ferromagnetic (FM) configurations. The total energy variation, which is taken as function of volume for both non-magnetic and ferromagnetic states with different concentrations, is illustrated in Fig. 2. It can be seen that these alloys are ferromagnetic. The results for Cu_2MnAl compound, which are given in Table I, agree with the experimental results [23,24] and other theoretical works [8, 10, 11, 25]. To the best of our knowledge, no comparable studies in literature on $Cu_2MnSi_{1-x}Al_x$ ($x = 0.125, 0.25, 0.375, 0.5$) alloys. The estimated lattice parameters (\AA), from the Vegard's law [26] in Eq. (1), for the

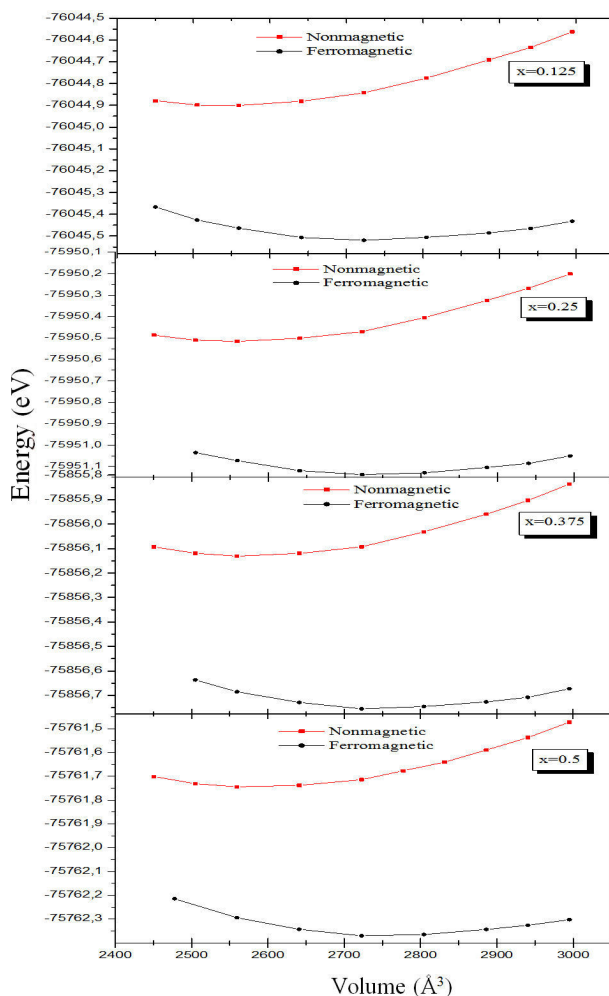


FIGURE 2. Calculated total energy as a function of volume curves for $Cu_2MnSi_{1-x}Al_x$ ($x = 0.125, 0.25, 0.375, 0.5$) alloy.

TABLE I. Calculated lattice parameter (a), bulk modulus (B) and its pressure derivative (B') for $\text{Cu}_2\text{MnSi}_{1-x}\text{Al}_x$ ($x = 0, 0.125, 0.25, 0.375, 0.5, 1$).

Compound	a (Å)	B (GPa)	B'
Cu_2MnSi	5.8645	136.137	5.147
$\text{Cu}_2\text{MnSi}_{1-0.125}\text{Al}_{0.125}$	5.87	118.758	6.136
$\text{Cu}_2\text{MnSi}_{1-0.25}\text{Al}_{0.25}$	5.88095	124.910	3.450
$\text{Cu}_2\text{MnSi}_{1-0.375}\text{Al}_{0.375}$	5.8879	126.467	4.229
$\text{Cu}_2\text{MnSi}_{1-0.5}\text{Al}_{0.5}$	5.8918	118.944	6.261
Cu_2MnAl	5.9274	126.689	4.066
Theo. [8,11,27]	5.962 [8]		
	5.957 [11]	115.64 [11]	
	5.915 [27]		
Exp. [24]	5.948 [24]		

TABLE II. Calculated elastic constants (in GPa), and G, B/G, E, ν , A, ξ of $\text{Cu}_2\text{MnSi}_{1-x}\text{Al}_x$ ($x = 0, 0.125, 0.25, 0.375, 0.5, 1$).

Compound	C_{11}	C_{12}	C_{44}	B	G	B/G	E	ν	A	ξ
Cu_2MnSi	133.423	138.671	108.124	137.029	63.824	2.146	165.740	0.319	-41.201	1.025
$\text{Cu}_2\text{MnSi}_{1-0.125}\text{Al}_{0.125}$	155.607	129.243	103.390	137.994	47.485	2.90	173.682	0.312	7.843	0.882
$\text{Cu}_2\text{MnSi}_{1-0.25}\text{Al}_{0.25}$	154.061	129.182	99.346	137.417	45.382	3.027	167.508	0.318	7.986	0.888
$\text{Cu}_2\text{MnSi}_{1-0.375}\text{Al}_{0.375}$	200.123	115.834	111.110	143.903	70.485	2.017	209.953	0.279	2.636	0.690
$\text{Cu}_2\text{MnSi}_{1-0.5}\text{Al}_{0.5}$	202.463	124.960	111.640	150.976	73.096	2.065	209.332	0.291	2.880	0.721
Cu_2MnAl	137.867	122.284	108.790	127.645	68.391	1.866	174.081	0.295	13.962	0.922
Theo. [11,25]	137.68[11]	104.61[11]	460.41[11]	115[11]						0.83[11]
	137 [25]	115 [25]	112 [25]	122[25]						0.89[25]
Exp. [23]	135.5[23]	97.3[23]	94 [23]							

selected concentrations 0.125, 0.25, 0.375, 0.5, are 5.86875, 5.8775, 5.88625 and 5.895 respectively.

$$\text{Cu}_2\text{MnSi}_{1-x}\text{Al}_x : a(\text{Å}) = 5.86 \times (1 - x) + 5.93 \times x \quad (1)$$

4.2. Elastic Properties

In order to discuss the mechanical stability of the parent compounds Cu_2MnSi , Cu_2MnAl and $\text{Cu}_2\text{MnSi}_{1-x}\text{Al}_x$ quaternary alloy, we have calculated the three independent elastic constants for cubic crystals C_{11} , C_{12} and C_{44} , by using a numerical first-principles method. The traditional mechanical stability conditions in cubic crystal are expressed as follows: $C_{11} - C_{12} > 0$, $C_{11} > 0$, $C_{44} > 0$, $C_{11} + 2C_{12} > 0$ and $C_{12} < B < C_{11}$ [28]. The calculated elastic constants C_{ij} , given in Table II, show that with the exception of Cu_2MnSi which does not fulfill the stability criteria, Cu_2MnAl and $\text{Cu}_2\text{MnSi}_{1-x}\text{Al}_x$ alloys are elastically stable. The obtained results for Cu_2MnAl alloy agree with experimental results in Ref. 23 and those of Rai *et al.*, [11] and Jalilian [25].

In addition, other parameters have been calculated as the Shear modulus (G), Young's modulus (E), Poisson's ratio (ν), anisotropy factor (A), and Kleinman parameter (ξ), listed in

Table II too. For these calculations, we have used the following equations:

$$G = \frac{G_R + G_V}{2} \quad (2)$$

$$G_V = \frac{C_{11} - C_{12} + 3C_{44}}{5} \quad (3)$$

$$G_R = \frac{5(C_{11} - C_{12})C_{44}}{4C_{44} + 3(C_{11} - C_{12})} \quad (4)$$

$$E = \frac{9BG}{3B + G} \quad (5)$$

$$\nu = \frac{3B - 2G}{2(3B + 2G)} \quad (6)$$

$$A = \frac{2C_{44}}{C_{11} - C_{12}} \quad (7)$$

$$\xi = \frac{C_{11} + 8C_{12}}{7C_{11} + 2C_{12}} \quad (8)$$

where G_V and G_R are Voigt's shear modulus and Reuss's shear modulus corresponding to the upper and the lower bound of G values respectively.

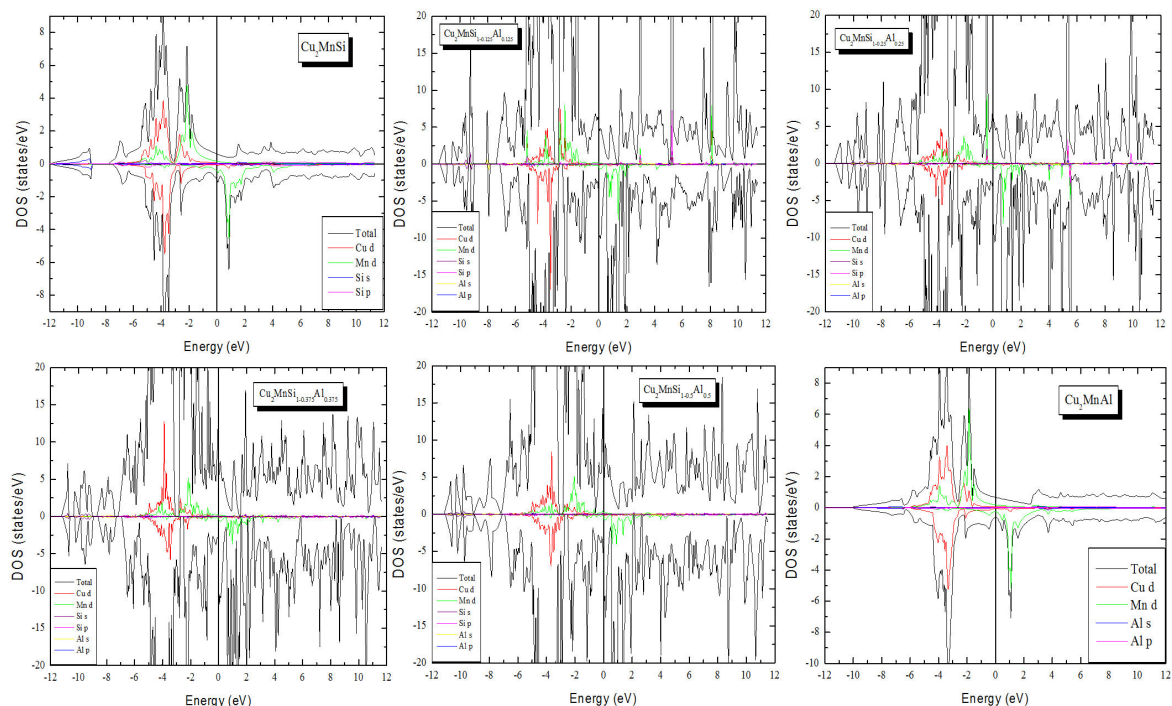


FIGURE 3. Total and partial density of states for $\text{Cu}_2\text{MnSi}_{1-x}\text{Al}_x$ ($x = 0, 0.125, 0.25, 0.375, 0.5, 1$) Heusler alloy.

Pugh [29] proposed an approximate criterion by the ratio B/G to predict the ductility of materials. If B/G ratio is higher than the critical value that separates brittle and ductile materials which is about 1.75, this corresponds to ductile behavior; else, the material is brittle. The calculated values in Table II indicate that the B/G ratios are between 1.866 and 3.027, suggesting the ductile nature of the studied alloys. The Cauchy pressure $C_{12} - C_{44}$ identifies the type of bonding [30]. Negative Cauchy pressure corresponds to more directional and non-metallic character, while positive value indicates predominant metallic bonding. According to Cauchy pressure, the predominant bonding for $\text{Cu}_2\text{MnSi}_{1-x}\text{Al}_x$ Heusler alloys is metallic. The Young's modulus (E) characterizes the stiff-

ness of a material. A higher value of E , stiffer is the material. It can be seen, from Table II, that Cu_2MnAl is stiffer than Cu_2MnSi . Poisson's ratio (ν) indicates the degree of directionality of the covalent bonds. Its value for covalent materials is small ($\nu < 0.1$), whereas the typical value for ionic materials is 0.25 [31]. Our calculated Poisson's ratios are from 0.279 to 0.319, so the contribution in the intra-atomic bonding for $\text{Cu}_2\text{MnSi}_{1-x}\text{Al}_x$ alloys is ionic. For an isotropic material, the anisotropy factor (A) is equal to one, while any different value shows anisotropy. The calculated anisotropy factor indicates that $\text{Cu}_2\text{MnSi}_{1-x}\text{Al}_x$ compounds are anisotropic.

TABLE III. Calculated total and partial spin magnetic moments (in μ_B) of $\text{Cu}_2\text{MnSi}_{1-x}\text{Al}_x$ ($x = 0, 0.125, 0.25, 0.375, 0.5, 1$).

Compound	M^{Cu}	M^{Mn}	M^{Si}	M^{Al}	$M^{\text{interstitial}}$	M^{tot}
Cu_2MnSi	0.067	3.305	-0.0062	—	0.302	3.735
$\text{Cu}_2\text{MnSi}_{1-0.125}\text{Al}_{0.125}$	0.073	3.332	-0.00002	-0.028	0.314	3.790
$\text{Cu}_2\text{MnSi}_{1-0.25}\text{Al}_{0.25}$	0.070	3.330	-0.00429	-0.030	0.302	3.762
$\text{Cu}_2\text{MnSi}_{1-0.375}\text{Al}_{0.375}$	0.063	3.297	-0.0071	-0.032	0.279	3.686
$\text{Cu}_2\text{MnSi}_{1-0.5}\text{Al}^{0.5}$	0.060	3.273	-0.0085	-0.033	0.262	3.636
Cu_2MnAl	0.047	3.242	—	-0.034	0.200	3.502
Theo. [8,11,23,33]	0.05 [8]	3.40 [8]		-0.07 [8]		3.47 [8]
		3.53 [11]				3.56 [11]
						3.51 [23]
	0.073 [33]	3.49 [33]		-0.046 [33]		3.73 [33]
Exp. [34]						3.6 [34]

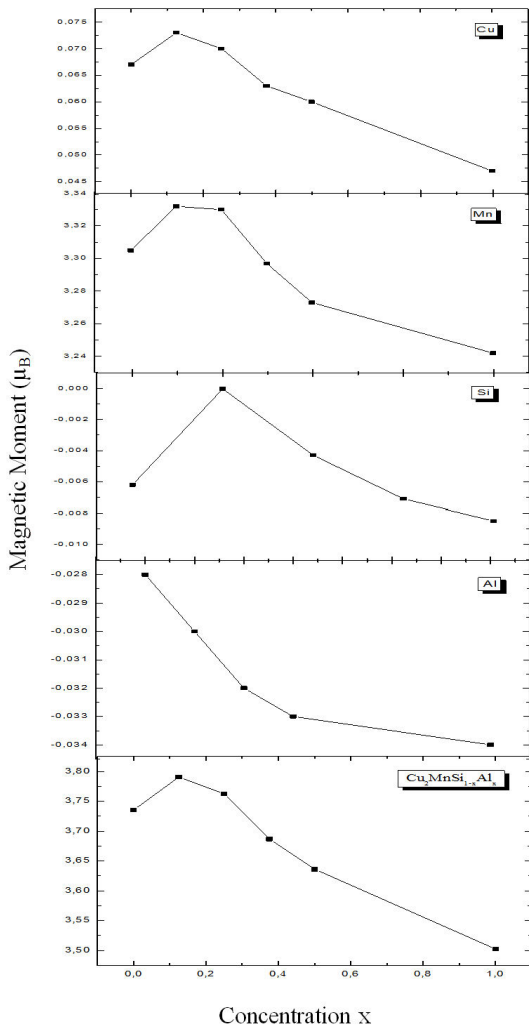


FIGURE 4. Magnetic moment for Cu, Mn, Si, Al and total magnetic moment within the concentration x for $\text{Cu}_2\text{MnSi}_{1-x}\text{Al}_x$ ($x = 0, 0.125, 0.25, 0.375, 0.5, 1$).

4.3. Electronic Properties

To determine the electronic structure's nature of $\text{Cu}_2\text{MnSi}_{1-x}\text{Al}_x$ compounds, we have calculated the total and partial densities of states for spin-up and spin-down, as displayed in Fig. 3. From this figure, one can see that there is no energy gap at Fermi level in both minority and majority spin states, proving the metallic character of the system. The TDOS spectrum of the parent compounds is divided into two main regions. The lowest valence bands below -9 eV for Cu_2MnSi (below -6 eV for Cu_2MnAl) are entirely due to Si and Al s-states, while the bands from -7 to 3 eV for Cu_2MnSi (-5.5 to 3 eV for Cu_2MnAl) are

chiefly governed by the Cu and Mn 3d states. A comparison with other studies obtained by Kulkova *et al.*, [8] and Rai *et al.*, [11], our results for Cu_2MnAl show quite good agreement. For $\text{Cu}_2\text{MnSi}_{1-x}\text{Al}_x$ quaternary alloy, the principally parts of the total densities of states situated between -5 to 3 eV, are contributed by the 3d states of Cu and Mn atoms.

4.4. Magnetic Properties

The calculated total and partial spin magnetic moments for Cu_2MnSi , Cu_2MnAl and $\text{Cu}_2\text{MnSi}_{1-x}\text{Al}_x$ quaternary alloy are quoted in Table III. Obviously, for Cu_2MnSi and Cu_2MnAl alloys, the total magnetic moment, which includes the contribution from the interstitial region, originates mainly from the Mn atom, with a small contribution of Si, Al and Cu sites. Our results agree well with Kulkova *et al.*, [8], Ghosh *et al.*, [13] and Kandpal *et al.*, [32]. For all the considered concentrations x , the positive spin magnetic moment of Cu and Mn means a ferromagnetic coupling between Cu and Mn atoms. The negative magnetic moment for Si and Al leads to an antiferromagnetic alignment of Si and Al ones. The obtained total and partial spin magnetic moment for the Cu_2MnAl alloy are in good agreement with previous theoretical results [8,11,32,33] and experimental ones [34], which are also reported in Table III. To our knowledge, there are no values of the magnetic moments in the literature for the quaternary alloy. In Fig. 4, the variation of the total and partial magnetic moments for $\text{Cu}_2\text{MnSi}_{1-x}\text{Al}_x$ ($x = 0, 0.125, 0.25, 0.375, 0.5, 1$) alloys versus the composition x , are non-linear.

5. Conclusion

In conclusion, using the FP-LAPW based on GGA approximations calculations to predict the structural parameters, elastic, electronic and magnetic properties of the $\text{Cu}_2\text{MnSi}_{1-x}\text{Al}_x$ quaternary alloy, we have found that the lattice constants are in excellent agreement with the estimated values by Vegard's law. The analysis of the electronic band structures and density of states of $\text{Cu}_2\text{MnSi}_{1-x}\text{Al}_x$ alloys reveal that they are ferromagnetic and metallic compounds by nature. The large magnetic moment is located on Mn sites. We have also found that the Cu_2MnSi does not fulfill the mechanical stability conditions, where Cu_2MnAl and $\text{Cu}_2\text{MnSi}_{1-x}\text{Al}_x$ Heusler alloys are stable and have a ductile behavior. The Young's modulus, Shear modulus, Poisson's ratio anisotropy factor and Kleinman parameters, often measured for polycrystalline samples, were also derived. We hope that this simulation may be a guideline for the experimentalists.

1. C. Felser, G.H. Fecher, and B. Balke, *Angew. Chem. Int. Ed.* **46** (2007) 668.
2. J. Winterlik, G.H. Fecher, and C. Felser, *Solid State Commun.* **145** (2008) 475.
3. K. Ullakko, J.K. Huang, C. Kantner, R.C. O' Handley, and V.V. Kokorin, *Appl. Phys. Lett.* **69** (1996) 1966.
4. A. Ayuela, J. Enkovaara, K. Ullakko, and R.H. Nieminen, *J. Phys.: Condens. Matter.* **11** (1999) 2017.
5. R.A. Dunlap, G. Stroink, and K. Dini, *J. Phys. F: Met. Phys.* **16** (1986) 1083.
6. P.J. Webster, and K.R.A. Ziebeck, *J. Phys. Chem. Solids.* **34** (1973) 1647.
7. S. Ishida, J. Ishida, S. Asano, and J. Yamashita, *J. Phys. Soc. Jpn.* **45** (1978) 1239.
8. S.E. Kulkova, S.V. Ereemeev, T. Kakeshita, S.S. Kulkov, and G.E. Rudenski, *Mater. Trans.* **47** (2006) 599.
9. K.H.J. Buschow, and P.G. van Engen, *J. Magn. Magn. Mater.* **25** (1981) 90.
10. Y.V. Kudryavtsev *et al.*, *J. Appl. Phys.* **97** (2005) 113903-1.
11. D.P. Rai, and R.K. Thapa, *J. Alloys. Compd.* **612** (2014) 355.
12. B. Hamri *et al.*, *Comput. Condens. Matter.* **3** (2015) 14.
13. S. Ghosh, and D.C. Gupta, *J. Magn. Magn. Mater.* **411** (2016) 120.
14. I. Galaknakis, *J. Phys.: Condens. Matter.* **16** (2004) 3089.
15. S.V. Karthik, and A. Rajanikanth, *Appl. Phys. Lett.* **89** (2006) 052505-1.
16. D. Nanto, D.S. Yang, and S.C. Yu, *Physica B.* **435** (2014) 54.
17. J.C. Slater, *Adv. Quant. Chem.* **1** (1964) 5564.
18. P. Blaha, K. Schwartz, G.K.H. Madsen, D. Kvasnicka and J. Liutz, *WIEN2k An Augmented Plane Wave Plus Local Orbitals Program for calculating Cristal Properties* (Vienna University of Technology, Vienna, Austria, 2001).
19. P. Hohenberg, and W. Kohn, *Phys. Rev. B.* **136** (1964) 864.
20. W. Kohn, and L.J. Sham, *Phys. Rev. A.* **140** (1965) 1133.
21. J.P. Perdew, K. Burke, and M. Ernzerhof, *Phys. Rev. Lett.* **77** (1996) 3865.
22. F.D. Murnaghan, *Proc. Natl. Acad. Sci. U S A.* **30** (1944) 244.
23. E.D.T. de Lacheisserie, D. Gignoux, and M. Schlenker, *Magnetism: Fundamentals* (Springer Science, Boston, USA, 2005).
24. R. Topkaya *et al.*, *J. Supercond. Novel. Magn.* **25** (2012) 2605.
25. J. Jalilian, *J. Alloys. Compd.* **626** (2015) 277.
26. L. Vegard, *Z. Phys.* **5** (1921) 17.
27. P. Entel, W.A. Adeagbo, A.T. Zayak, and M.E. Gruner, *NIC Symposium*; G. Münster, D. Wolf and M. Kremer, Eds. (NIC Series, Jon von Neumann Institute for Computing, Jülich, Germany, 2006), pp. 159-166.
28. G.V. Sin'ko, and N.A. Smirnov, *J. Phys. Condens. Matter.* **16** (2004) 8101-8104.
29. S.F. Pugh, *Philos. Mag.* **45** (1954) 823.
30. D.G. Pettifor, *Mater. Sci. Technol.* **8** (1992) 345.
31. J. Haines, J.M. Léger, and G. Bocquillon, *Annu. Rev. Mater. Res.* **31** (2001) 1.
32. H.C. Kandpal, G.H. Fecher, and C. Felser, *J. Phys. D, Appl. Phys.* **40** (2006) 1507.
33. S. Ishida, Y. Kubo, J. Ishida, and S. Asano, *J. Phys. Soc. Jpn.* **48** (1980) 814.
34. R. Caroli, and A. Blandin, *J. Phys. Chem. Solids.* **27** (1966) 503.